An Integrated Approach to Modelling the Fluid-Structure Interaction of a Collapsible Tube.

Scroggs, R.A., Beck, S.B.M., and Patterson, E.A.,

Corresponding author: Dr Stephen Beck, Department of Mechanical Engineering, The University of Sheffield, Mappin street, Sheffield, S.Yorks, S1 3JD, UK.

Fax (0)44 144 2227890

E-Mail s.beck@shef.ac.uk

Summary

The well known collapsible tube experiment was conducted to obtain flow, pressure and materials property data for steady state conditions. These were then used as the boundary conditions for a fully coupled fluid-structure interaction (FSI) model using a propriety computer code, LS-DYNA. The shape profiles for the tube were also recorded.

In order to obtain similar collapse modes to the experiment, it was necessary to model the tube flat, and then inflate it into a circular profile, leaving residual stresses in the walls. The profile shape then agreed well with the experimental ones.

Two departures from the physical properties were required to reduce computer time to an acceptable level. One of these was the lowering of the speed of sound by two orders of magnitude which, due to the low velocities involved, still left the mach number below 0.2. The other was to increase the thickness of the tube to prevent the numerical collapse of elements. A compensation for this was made by lowering the Young's modulus for the tube material.

Overall the results are qualitatively good. They give an indication of the power of the current FSI algorithms and the need to combine experiment and computer models in order to maximise the information that can be extracted both in terms of quantity and quality.

Nomenclature

c	speed of sound through material	m s^{-1}
E	Young's modulus	MPa
P	pressure	Pa
P_{12}	pressure difference between ends of pipe	Pa
P_{E1}	upstream transmural pressure	Pa
P_{E2}	downstream transmural pressure	Pa
Q	volumetric flow rate	m^3 s^{-1}

Subscripts

1	Upstream end of flexible tube
2	Downstream end of flexible tube
E	Sealed container around tube

1. Introduction

Many of the vessels which carry fluid in the human body are elastic and can collapse when the transmural (difference between internal and external) pressure falls below a critical value. This phenomenon of a flexible tube with an external pressure and a fluid flow has been studied by various researchers starting in 1914 when Starling [1] employed a thin-walled collapsible tube as a hydraulic analogue for a vein in a canine heart-lung preparation. Thirty years later Holt [2] investigated how the collapse of veins might affect peripheral venous pressure. He set up a model where water flowed through a rigid pipe to a collapsible segment of thin-walled rubber tubing and out through a more rigid pipe.

Conrad [3] first presented systematic experimental pressure flow curves for both steady and unsteady flow conditions of a Penrose tube, which is a thin-walled latex rubber tube. Many researchers have since used this standard set-up and variations on it. He described three general states which can be categorised by viewing the cross-sectional profile at the pinch, which occurs near the downstream end of the tube. The various profiles are shown in Figure

1. In states 1 and 3 the tube behaves like a laminar flow resistance whose value in state 1 is much larger than in state 3 because of the difference in cross-sectional areas. The other states reflect the delicate balance between stresses in the wall and the transmural pressure distribution. The changing resistance of the geometry of the tube causes the pressure-flow relationship to be non-linear and it is between these states that instabilities can occur. These instabilities are self-excited oscillations; a phenomenon that causes collapsible tube models to be complicated to simulate. In steady-state, the response of the shape of the tube can be characterised by flows or pressure differences.

Katz et al [4] described the volume within a collapsible tube as a function of transmural pressure P_{EI}. He treated the geometry seen in states 1 and 3 as constant, since large changes in transmural pressure result in small changes of volume. In between these states the tube appears to be more flexible, and small changes in transmural pressure can substantially change the geometry and hence volume of the tube.

There has been a lot of interest in the modelling of these systems, and prior to the introduction of computer codes that would deal with full fluid-structure interaction (FSI), finite element codes were used to model both the tube shape and stresses within its walls. However recently the collapsible-tube phenomenon has been modelled two-dimensionally by Rast [5] who used a section of rigid channel with a section of thin-walled membrane. A steady-response result was obtained with the governing equations of the fluid simultaneously solved with the elastic membrane equations for the structure. Luo and Pedley [6] carried out similar work when they used the commercially available finite element code FIDAP for steady flow in a two-dimensional collapsible channel. This work was complemented by the independent development of a time-dependent simulation of the coupled flow-membrane problem, [7] with which oscillations of the tube geometry were observed.

Heil [8] successfully attempted the three-dimensional modelling of a collapsible tube when he coupled non-linear shell theory with the three-dimensional Stokes equations to analyse the slow viscous flow through a compliant tube. His results included the fluid flow field in the tube and the tube deformation for several sets of boundary conditions.

Tang et al [9] used ADINA to model wall stress and strain with FSI for blood flow in stenotic arteries although, again, the deformations of the structure were not large. Bathe and Kamm [10]produced a similar model for pulsatile flow through a stenotic artery although this was a two-dimensional model.

The objective of the work presented is to use a proprietary FSI code for the simulation of the three dimensional behaviour of a collapsible tube and to integrate the analysis with physical experiments in order to inform and verify the simulation.

2. Numerical Formulations for Fluid-Structure Interaction

Conventionally, finite element formulations use a Lagrangian mesh, which is fixed to the structure and therefore moves with it. There is no movement of matter through the mesh. Therefore Lagrangian methods are well suited to maintaining material interfaces. In a fluid analysis Lagrangian meshes are generally limited to small displacement problems such as sloshing, as the representation of large deformations is hindered by shear and vorticity which tends to tangle the mesh. In the Eulerian simulations normally used in fluids codes, the mesh is fixed in space and the fluid moves from one cell to another thus avoiding any distortion. However, these are unsuitable for free surface or fluid-structure interaction problems.

The arbitrary Lagrangian-Eulerian (ALE) formulation is a relatively new tool first published by Hirt et al [11] and has, so far, mainly been used in crash analysis and metal forming. The essence of the ALE idea is that the mesh motion can be chosen arbitrarily, providing

additional flexibility and accuracy. The method uses a mesh with vertices that can either move with the fluid (Lagrangian), be held fixed (Eulerian), or displace in any other prescribed way.

LS-DYNA is an explicit three-dimensional finite element code which was designed for analysing the large-deformation dynamic response of structures [12]. Recently, this has also included structures coupled to fluids using the ALE formulation. The analyses presented in this work use version 950d of this code.

The fluid modelled in the Eulerian mesh must be able to interact with the structure defined by the Lagrangian mesh. Coupling is the method which computes the interaction of the two sets of elements. Pressure forces from the Eulerian flow mesh load the Lagrangian mesh at the boundaries. The resulting Lagrangian deformation then influences the fluid flow in the Eulerian mesh. This process is simplified in LS-DYNA since both Eulerian and Lagrangian parts follow the same explicit Lagrangian time-step. At the end of the time-step the Eulerian mesh is remapped while the Lagrangian structure remains deformed. By viewing the transient results of an Eulerian-Lagrangian coupling it appears that a fluid is moving through a spatially fixed mesh and deforming a structure defined by a separate mesh embedded within it.

The CPU cost of an LS-DYNA analysis is controlled by the number of elements in the model, the complexity of the model geometry and the time-step, which is the period of time between updates of the model parameters. A small time-step is undesirable since it will result in more computational cycles before the simulation is finished. The control of the time-step is therefore an effective way of lowering the CPU time. LS-DYNA automatically calculates the largest time-step that can be used without triggering numerical instability. The criterion used is the time of flight for a sound wave across the smallest element in the mesh.

3. Experimental Details

The basic premise for the experiment was to have a length of flexible tubing with a pressure at either end, provided by tanks whose constant head could be varied by altering their height above the tube. The tube was a piece of standard latex Penrose tubing conventionally used in medical applications. This tube needed an external pressure on it. To this end, the tube was mounted in a sealed glass container (300×300×190 mm) which could be pressurised using a third tank.

The flow rate was measured using Rotameter type flowmeters. The flow was controlled using valves on either side of the sealed container. Pressures transducers were fitted between the valves and the tank and a third was fitted to measure the pressure in the container (Figure 2).

The plane of collapse of the tube was determined by the residual stresses due to manufacture and flat packing. The tube was installed in the apparatus so that the plane of flat packing was horizontal. The 13 mm diameter tube was stretched onto the 17 mm diameter inlet and outlet sections so that there was no visible twist in the tube walls. The tube was 67 mm long, and the gap between the rigid inlet and outlet sections was 65 mm. The extra 2 mm was taken up by the axial tension caused by the mounting points being of a larger diameter than that of the undeformed tube. The pressure container was then sealed and filled with water.

For each family of experiments, the pressure difference between the inlet and the sealed container ($P_1 - P_e$) were fixed at a value between 100 and 800 Pa, and the pressure difference between the inlet and the outlet of the tube ($P_1 - P_2$) was recorded for a variety of flow rates which varied between zero and 2×10^{-6} m^3 sec^{-1}.

Video footage of the experiment was obtained from both the top and side of the flow domain.

The physical dimensions of the tube were measured using Vernier callipers and a ruler. Great care was taken to avoid compressing the material. The Poisson's ratio for the tube was obtained from standard references as 0.5, which means that the tube was of constant volume. The of the material was obtained by measuring the force/displacement curve of samples of the tube and was found to be 1.3 MPa. The material was measured both along and across the tube and was found to be isotropic. A correction had to be applied when calculating the Young's modulus, as the material got thinner as it was stretched.

4. Computational Details

The soft structure and high level of interaction with the fluid flow prohibits the detailed measurements required to quantify local stress and flow parameters for the tube. Consequently, numerical simulations can play an important rôle in providing detailed data that is necessary to inform our understanding of the behaviour of the tube. As far as was possible, the numerical model was to mimic the experiment described above and hence the boundary conditions, tube material properties and geometry were taken from the experiment.

These analyses are very computer intensive, and it was not possible to produce a full set of results for grid independence such as in a convergence study, so the mesh size was determined based on analysis of small portions of the flow domain. A minimum mesh size for the solid is required to prevent the flow passing through it, as experience has shown that it will have a porosity dependent on the relative mesh densities of the fluid and structure domains.

To avoid excessive CPU run times, it was necessary to raise the time-step by lowering the speed of sound, c, in the equation of state. This approach was used because the time step is calculated as the time of flight across the smallest element in the mesh. The size of the mesh is constrained by the need to achieve accurate results and to avoid porosity in the structure.

The consequence, or side effect of accelerating the computational times in this manner is that the fluid becomes more compressible. However, the effects of fluid compressibility in this particular analysis initially were deemed to be negligible. Tests on a simple system showed that the value of wall shear stress was found to differ by 0.7% as the speed of sound was varied between c = 30 and 60 m s^{-1}. Even with this change, some of the computational runs took up to a week on a 300 MHz Sun workstation.

LS-DYNA allows the user to define the solid and fluid domains separately and then to mesh them together. Unlike most FSI packages which are fluid based, LS-DYNA was developed from a time stepping solid modelling code. The solid modelling portions of the program are well validated, but the fluid modeller, and hence the FSI portions are still relatively new additions. This well developed solid modelling capability means that it is possible to perform operations on the tube that are the direct analogue of those performed in the experiment. Thus the model was constructed from a series of different sections that were then assembled and boundary conditions applied.

4.1. Modelling Details

The fluid and structural parts of the model were created simultaneously in HYPERMESH. The coupled FE model was then imported into LS-DYNA with additional editing carried out manually as needed.

The fluid mesh had rigid inlet and outlet sections and a main flow domain which surrounded the tube; and was modelled using 79956 eight-noded elements. At the ends of the rigid sections were reservoirs. The fluid domain was essentially cylindrical with an equatorial extension to accommodate the collapsed tube. This shape was more economical than using a larger diameter cylinder. The external pressure container was modelled as a reservoir of ambient Eulerian elements defined on the outer surface of the fluid domain in order to control

the pressure, P_E, and to add or remove fluid as required. The rigid inlet and outlet sections were defined with no-slip conditions on their walls.

The lengths of the edges of the elements normal to the flow were all less than 1 mm, and where contact of the tube wall with itself was observed in the experiments, these lengths were reduced to below 0.5 mm.

The flexible tube was modelled flat, as it was supplied (see Figure 3). This was an important part of the modelling, as the associated residual stresses meant that the tube would tend to collapse back to the flat form. Its structure was modelled using 9840 four-noded Belytschko-Lin-Tsay (BLT) shells. This type of shell was used, as even though they were computationally cheaper than corresponding brick elements, they were still able to model a variation in stress through the wall thickness which is important for the large deformations being simulated.

Once both domains had been meshed, it was necessary to fit the flexible tube onto the rigid inlet and outlet pipes. This was accomplished by applying displacement vectors to each row of nodes along the tube to move them into a circle. Then displacement loads were removed, except at the locations of the rigid inlet and outlet pipes. The flexible portion of the tube thus acted as if it were stretched onto the rigid inlet and outlet pipes. The material between the inlet and outlet was free from any additional forces except through its coupling with the fluid. This is shown in Figure 4.

When a cylinder is expanded in the radial direction, Poisson's ratio causes it to contract longitudinally if it is unconstrained and experience longitudinal tensile stress if it is constrained longitudinally. In the experiment, this effect was accounted for through the use of a 67mm long flexible tube which produced no axial tension when it was fitted into the 65mm gap between the rigid pipes. In the simulations, the expanding of the tube radially using

displacement loading effectively constrained it in the longitudinal direction. A longitudinal tensile stress was thus induced in the 65mm tube. To counteract this, an initial stress (−0.271 MPa) was introduced to so the tube a stress free tube when it was fitted to the rigid pipe.

The material was assumed to be linear elastic with a constant Young's modulus and the fluid was assumed to be Newtonian with the properties of water.

Preliminary results contained some evidence of deformation that induced zero strain energy; this unrealistic behaviour is caused by numerical instability when modelling large deformations and is known as hourglassing. It was removed by increasing the wall thickness from 0.35 to 0.5 mm. The force deflection characteristic was maintained by a corresponding decrease in Young's modulus from 1.3 to 0.91 MPa. This alteration to the stiffness characteristic is simpler and computationally cheaper than increasing the mesh density in order to achieve numerical stability.

The model was analysed using a range of values of the downstream transmural pressure P_{E2} (being 100, 400 and 800 Pa) and for two flow rates. Conditions for a collapsed tube were achieved using a low flow of 1.66×10^{-6} m^3 sec^{-1} and for compliant conditions using a higher flow rate of 8.3×10^{-6} m^3 sec^{-1}. The results from the simulation replicate the experiments with a high degree of similitude. This includes features such as the local decrease in tube diameter which occurs just downstream of the inlet and just upstream of the outlet (Figure 5). This is a consequence of the tube being stretched from a 13mm diameter to a 17 mm on the fixed end pipes. The vertical or top view of this feature shows it to be strongly localised at the outlet end since the diameter increases as the pinch point is approached.

Further refinement of the mesh resulted in unrealistic solution times. increases in the speed of sound in the fluid also slowed the solution to unacceptable levels, so it was decided that this configuration was the best that could be achieved within a reasonable time.

5. Results

5.1. Experimental Results

The results from the experiments are shown in Figure 6. Interpretation of these curves becomes far easier if the data is scaled. The pressure difference between the ends of the tube, P_{12}, which is plotted on the y-axis can be normalised by the upstream transmural pressure P_{E1} to produce a dimensionless quantity. The flow rate, Q can be multiplied by $\sqrt{P_{1E} \times \rho}$ which has the dimensions of force. The result of this is shown in Figure 7 and it will be seen that the curves all collapse neatly on to each other. The fact that the x-axis has the units of force implies that this scaled (though still dimensional) number is involved with the fluid-structure interaction, but more results are needed to find out which physical parameter from the solid portion of the experiment would render this quantity truly non-dimensional. Towards the origin, the transmural pressure is higher than the pressure drop along the tube and so the tube is fully collapsed. As the transmural pressure decreases, the tube opens out, and when it is about 103% of the pressure drop down the flexible portion, the tube is fully opened into a circular cylinder and the flow then increases with the pressure difference between the ends of the tube.

An example of the video stills obtained from the experiments are shown in the top half of Figure 5. It can be seen that, due to the residual stresses from the manufacturing and packing processes, the tube collapses to a horizontal flat profile corresponding to its initial state. It will also be seen that the pinched section is near the outlet. This is due to the pressure drop

along the tube causing the pressure to be lower near the outlet, leading to a greater transmural pressure at the outlet.

5.2. Computational Results

The pinch is well to the downstream end of the flexible tube, for the reason described in the experimental section.

The position of the pinch in relation to the outlet for both the computational and experimental models at a flow rate of 8.3×10^{-6} m^3 sec^{-1} are shown in Figure 8. The biggest difference was 0.95mm (5.6% of the outlet tube outer diameter) for a downstream transmural pressure, P_{E2} of 80 cmH_2O. The difference for the lower P_{E2} values was less than 0.35mm or 2% of the outlet tube outer diameter. It is not surprising that the largest discrepancy was measured at the largest value of P_{E2} since the larger strains associated with higher transmural pressures would be expected to magnify the effect of any imperfections in the modelling of the material properties and of the standard contact conditions.

One of the strengths of the computational technique is that it is relatively easy to obtain full field data. With full FSI, both the stresses in the solid and the flows in the fluid portions can be computed and displayed.

The velocity vectors for the flow are shown in Figure 9 for downstream transmural pressure P_{E2} of 80 cmH_2O and flow rates of 1.66×10^{-6}, 8.33×10^{-6} and 1.66×10^{-5} m^3 sec^{-1}. It will be seen that for the lowest flow rates, at the pinch, the flow goes down the two side channels left when the tube collapsed. On either side of the pinch, the area is greater, and thus the velocity drops. For the high flow rate, there is no pinch, and the pipe is circular. The flow thus accelerates through the reduced area near the outlet of the flexible portion. For the

intermediate condition, there is small pinch, and the flow accelerates through this portion and slows down as the area increases beyond the small pinch.

The choice of BLT shell elements with three integration points through their thickness allows the stresses through the wall of the tube to be calculated. Despite the thin-walled cross-section, bending stresses are present in the wall of the tube due to large changes in shape [13]. This is particularly evident around the pinch point and the outlet where the tube has been stretched onto the fixed pipe as shown in Figure 10 for the fully collapsed state. Examining the tightly radiused edges of the bottom figure with the top one shows the greater tension in the outside of the tube when compared to the inside.

6. Discussion

One of the primary aims of the work was to employ an integrated approach to studying the behaviour of a flexible tube subject both to internal flow and external pressure. The physical experiment has been used to provide boundary conditions for the computational model; whilst video footage of the shape of the tube has been used to validate the simulation. The simulation provides detailed data relating to wall stresses and flow velocities in the tube. This data is three-dimensional and potentially time-varying for unsteady conditions. The interaction of the fluid flow and soft structure make it impossible to measure the spatial variation of these quantities without radically altering the system and hence the parameters being assessed. Consequently the computer simulation integrated with the physical experiments creates a powerful tool for informing and extending our knowledge of this type of system.

The shapes of the tube shown in Figure 5 suggest good agreement between the experiment and simulation, although there are some minor differences. These differences are associated with the position (see Figure 8) and shape of the pinch. The reasons for these differences are

not known, although they might be a result of the assumption of linear stress-strain properties for the latex rubber from which the tube is manufactured. Rubber tends to behave as a non-linear elastic material, for which LS-DYNA has appropriate material models. However, the higher computational cost of these more sophisticated models was not acceptable given the already long computational times required for the simple linear model. The other source of the discrepancies could be the initial state of the tube which was received flat-packed and stretched to fit onto the rigid inlet and outlet pipes. This process of fitting was modelled in the simulation assuming that the flat-packed state is stress-free. The validity of this assumption is dependent on the precise details of the manufacturing process and once again direct measurement of the stresses is impractical. However, as can be deduced from Figure 8 the differences between the physical experiment and simulation are relatively small, thereby providing confidence in the simulation.

In preliminary models, the pre-forming was not simulated and the analysis commenced with the initial geometry of the tube corresponding to the fitted shape. From this starting state the tube either twisted or collapsed to a cross or cruciform state which did not correspond to the flat shape seen in the experiments. The preliminary models also highlighted the sensitivity to the bending behaviour of the tube wall. Thin-walled pressure vessels experience bending stresses when subjected to large-scale deformations leading to significant changes in curvature [13]. For this reason the BLT shell elements with through thickness integration points were used to model the tube wall. However, some hour-glassing occurred due to deformation without strain energy which is usually a computational artefact occurring as a result of a coarse mesh. Further refinement of the structural mesh would have lengthened the computational time prohibitively and so, instead, the bending stiffness was rendered larger, through increasing the wall thickness whilst simultaneously decreasing the Young's modulus in order to retain the tensile stiffness. This adjustment reduced the bending deformations, thus

eliminating the hour-glassing. However, the increased bending stiffness could be responsible for the source of the small differences in shape observable in Figure 5.

The other major physical difference between the experiment and the model that was forced on the authors was the lowering of the speed of sound in the model. As was stated above, this had to be done in order to reduce CPU times to a viable level. However, due to the low velocities within the experiment, the mach number was kept below 0.2, and could be deemed not to affect the results unduly. Typical times for analysis were one week of processor time on a 300 MHz workstation.

Though there is currently no turbulent flow model in LS-DYNA, for the models describe here, the flow was laminar throughout the flexible section. A turbulent modeller would be vital for many applications, but for the flexible tube experiment, a non-Newtonian viscosity formulation, which does exist but is computationally very intensive would allow the modelling of blood flow.

LS-DYNA is a time stepping program, and though steady state results have been shown here, they are the settled results of a dynamic study. Indeed, close examination of the shape of the flexible tube at the end of the an analysis showed small instabilities in the profiles, which is a similar effect to that seen in the experiment.

7. Conclusions

The value in using an integrated approach to the analysis of a collapsible tube has been shown. A physical experiment was used to obtain boundary conditions for the numerical model, and to provide shape profiles that were used to validate the model. The FSI model provided local three dimensional and potentially time varying data on the stress distributions and flow velocities in the tube, which could not be measured in the physical experiment. The

integrated approach allows data of greater quality and quantity to be obtained with greater confidence than the sole application of either numerical or experimental techniques. It is possible to recreate the results for a collapsible tube experiment using the explicit, time stepping code LS-DYNA. However, without the preforming of the tube, unrealistic modes of collapse were obtained from the computer model, due to the lack of residual stresses in the tube. This emphasizes the importance of simulating all stages in the experiment, including in this instance the setting-up procedure.

The large deformation of the tube involved changes in curvature which generate bending stress in the wall of the tube, so that it cannot be considered as a *thin walled structure* in the classical sense. The use of two dimensional shell or membrane elements is inappropriate and instead shells with through thickness integration points were used.

One major deviation from the actual experiment was required to lower CPU times to an acceptable level. This was to reduce the speed of sound to 10 ms^{-1} , which is a large change, but tests showed that only small differences in results would be obtained by using the true sonic velocity.

Further work to overcome the problems described above is continuing, as is modelling of the unstable modes. With further increases in computer power, the deviations from physicality could be removed and it will be possible to use the computer a design tool for fluid-structure interaction systems.

Acknowledgements

The authors gratefully acknowledge the assistance of Simon Wiles in helping to construct the experiment. They would also like to acknowledge the support of Arup and Partners and EPSRC for this work.

References

[1] PATTERSON, S. W. PIPER, H. & STARLING, E. H. The Regulation of the Heart Beat, *Journal of Physiology*, **Vol. 48** (1914), pp 465.

[2] HOLT, J. P. The Collapse Factor in the Measurement of Venous Pressure: The Flow of Fluid Through Collapsible Tubes, *American Journal of Physiology,* **Vol. 134** (1941, pp 292–299.

[3] CONRAD, W. A. Pressure-Flow Relationships in Collapsible Tubes, *IEEE Transactions on Bio-Medical Engineering*, **Vol. BME-16** (1969), pp 284–295.

[4] KATZ, A. I. CHEN, Y. & MORENO, A. H. Flow Through a Collapsible Tube: Experimental Analysis and Mathematical Model, *Biophysical Journal*, **Vol. 9**(1969, pp 1261–1279.

[5] RAST, M. P. Simultaneous Solution of the Navier-Stokes and Elastic Membrane Equations by a Finite Element Method, *International Journal for Numerical Methods in Fluids*, **Vol. 19** (1994), pp 1115–1135.

[6] LUO, X. Y. & PEDLEY, T. J. A Numerical Simulation of Steady Flow in a 2-D Collapsible Channel, *Journal of Fluids and Structures*, **Vol. 9**, (1995) pp 149–174.

[7] LUO, X. Y. & PEDLEY, T. J. A Numerical Simulation of Unsteady Flow in a Two-Dimensional Collapsible Channel, *Journal of Fluid Mechanics*, **Vol. 314 (**1996), pp 191–225.

[8] HEIL, M. Stokes Flow in Collapsible Tubes: *Computation and Experiment, Journal of Fluid Mechanics*, **Vol. 353** (1997), pp 285–312.

[9] TANG, D. YANG, C. HUANG, Y. & KU, D. N. Wall Stress and Strain Analysis Using a Three-Dimensional Thick-Wall Model With Fluid-Structure Interactions for Blood Flow in Carotid Arteries with Stenosis, *Computers and Structures*, **Vol. 72** (1999), pp 341–356.

[10] BATHE, M. & KAMM, R. D. A Fluid-Structure Interaction Finite Element Analysis of Pulsatile Blood Flow Through a Compliant Stenotic Artery, *ASME Journal of Biomechanical Engineering*, **Vol 121 (**1999), pp 361–369.

[11] HIRT, C. W. AMSDEN, A. A. & COOK, J. L. An Arbitrary Lagrangian-Eulerian Computing Method For All Flow Speeds, *Journal Of Computational Physics*, **Vol. 14** (1974), pp 227–253.

[12] HALLQUIST, J. 0. LS-DYNA Theoretical Manual, Livermore Software Technology Corp, Livermore, California (2000).

[13] CHEW, G. G. HOWARD I. C. & PATTERSON E. A. On the presence of bending stresses in inflated thin-walled structures, *Proceedings of the Institution of Mechanical Engineers-C*, **Vol. 211, N5** (1997). pp 341-348.

Figures

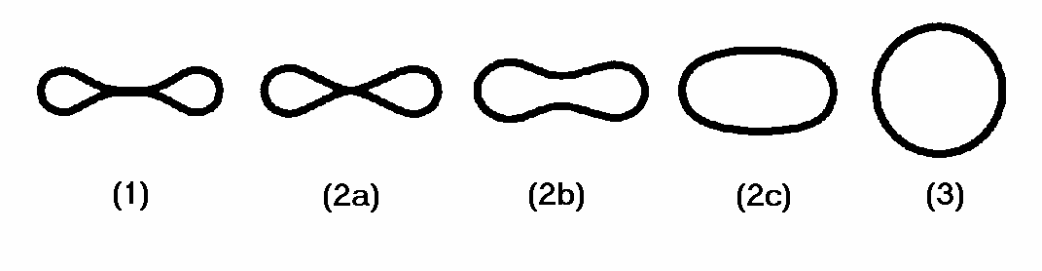

Figure 1. Cross sectional profiles at the neck or pinch point at various operating points on the characteristic curve 1) Line contact; 2) Highly compliant 3) Cylinder. After [3].

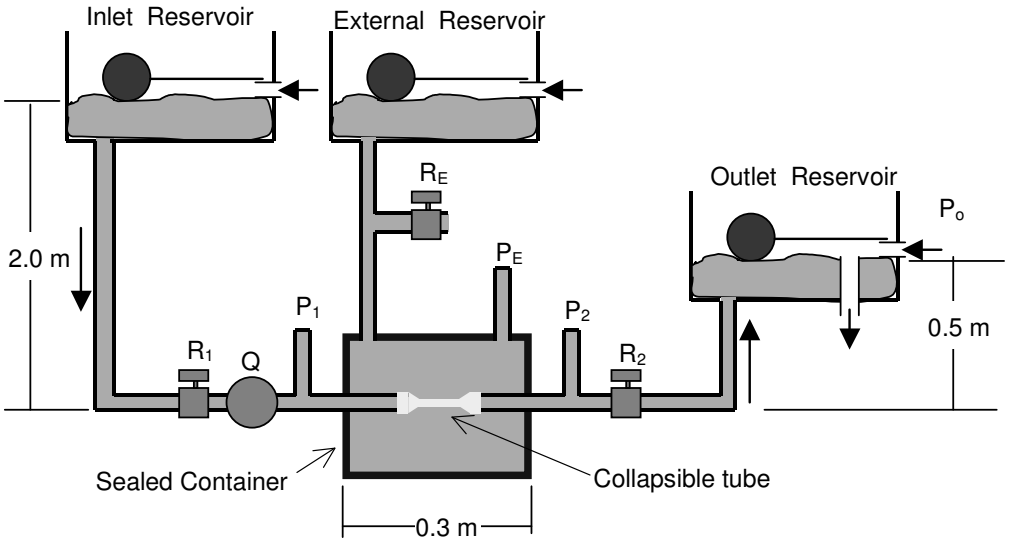

Figure 2. Schematic diagram of the experimental set-up used in the collapsible tube experiments.

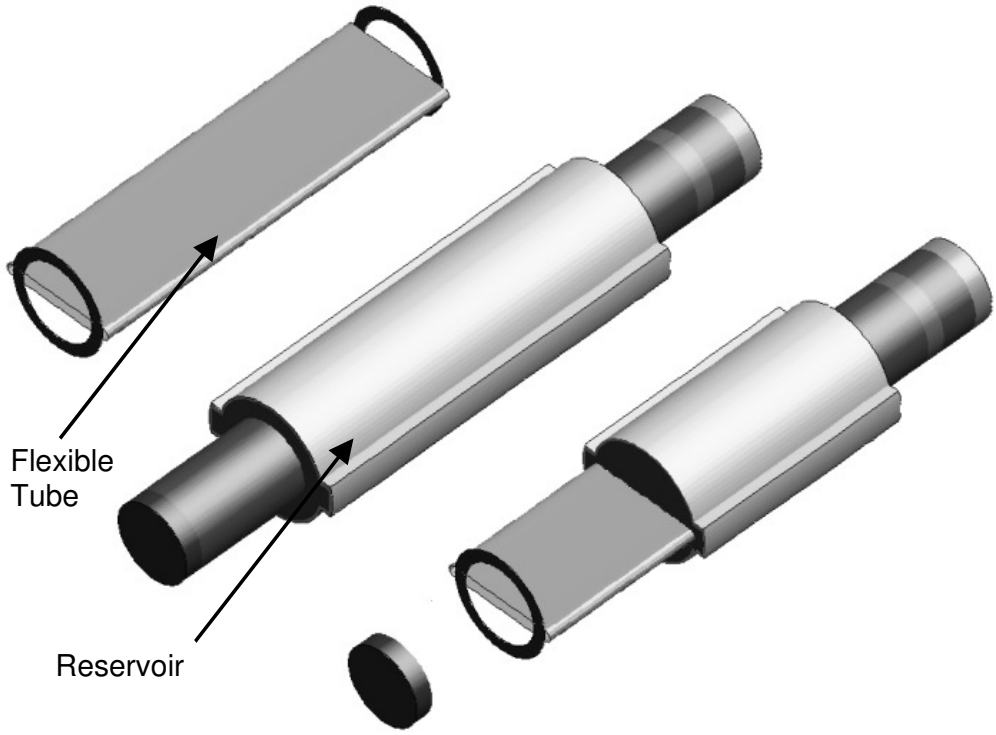

Figure 3. Structural (left), fluid (middle) and coupled (right) parts of the LS-DYNA model.

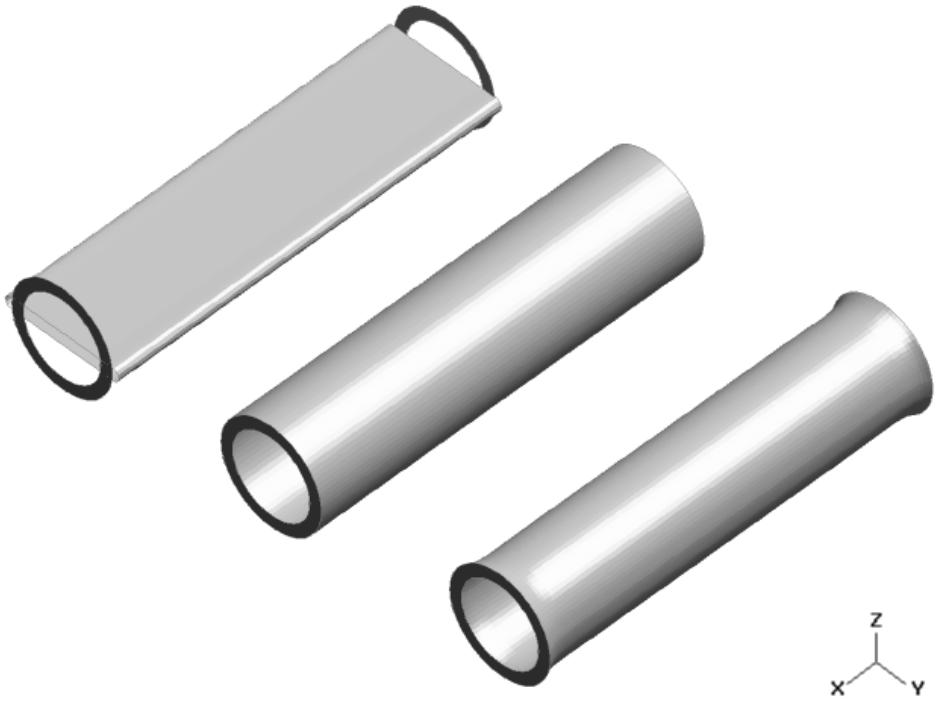

Figure 4. Preforming process for the collapsible tube. (a) tube in undeformed 'flat' state; (b) tube after the nodes have been displaced radially to form a circle; and (c) tube after removal of the displacement vectors except at the rigid inlet and outlet.

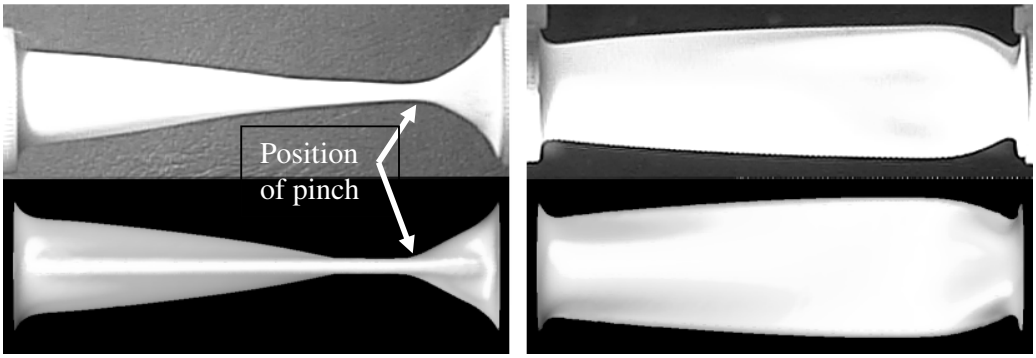

Figure 5. Vertical or side (left) and horizontal or top profiles (right) from experiment (top) and simulation (bottom) for the collapsible tubes ($Q = 8.3\times10^{-6}$ m^3 sec^{-1}, $P_{E2} = 100$ Pa). The flow direction is from left to right.

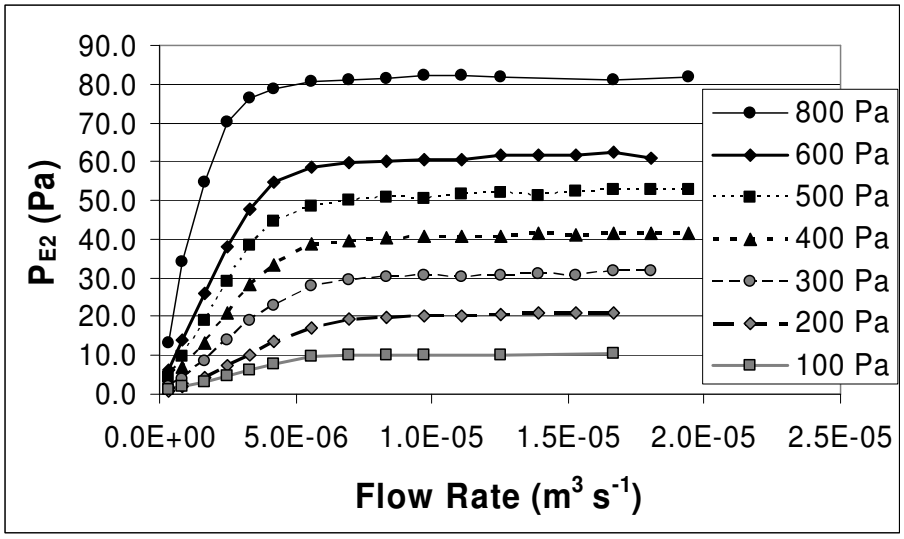

Figure 6. Family of characteristic curves for values of the downstream transmural pressure $P_E - P_2$ obtained from experiments

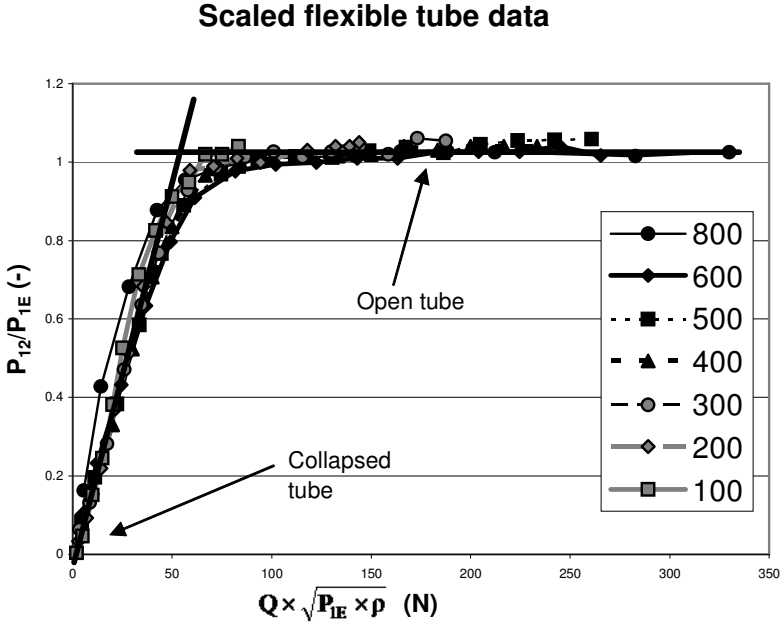

Figure 7. Scaled experimental data, based on the data in Figure 6 for various values of $P_E - P_2$ illustrating how the data can be superimposed by appropriate choice of normalising factors.

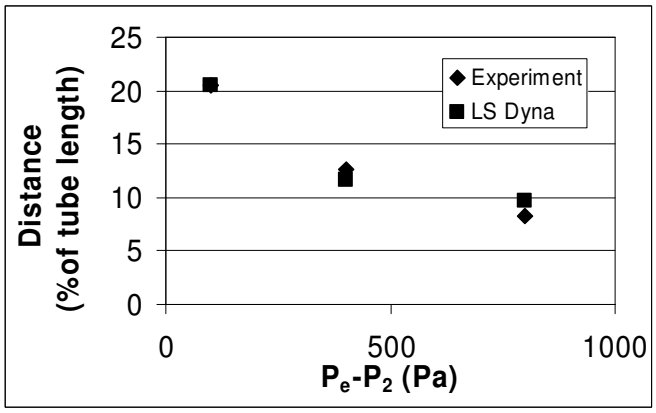

Figure 8. Comparison of experimental and simulation results for the distance from the outlet to the pinch for various container to outlet pressures (P_E-P_2) at a flow rate of 8.33×10^{-6} m^3/sec.

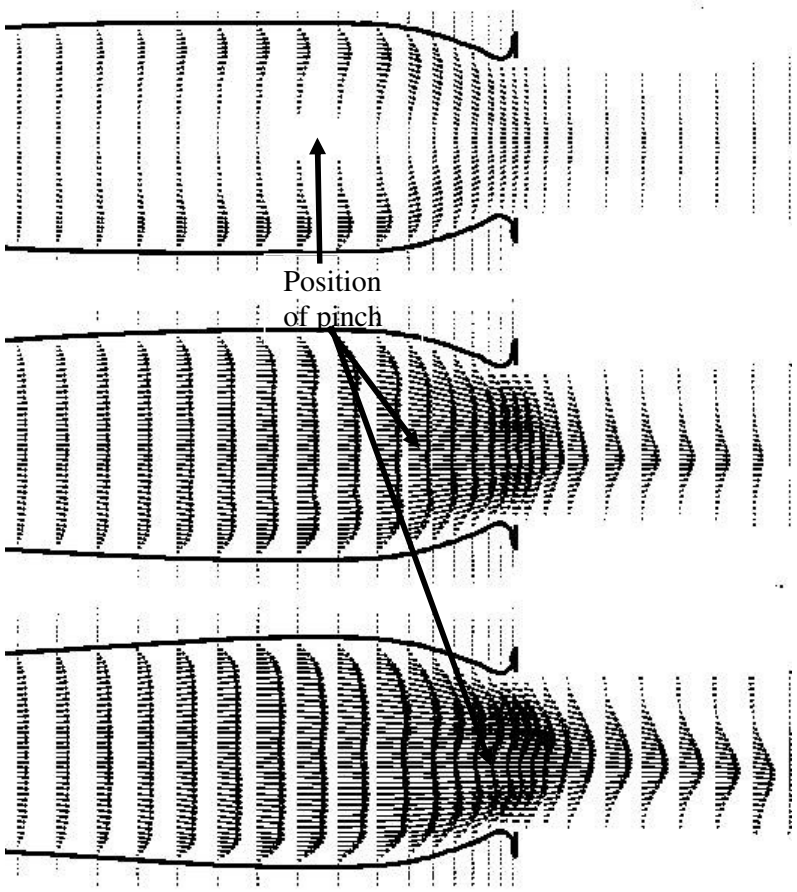

Figure 9. Top view of the central horizontal plane showing velocity vectors (mm/s) in the vicinity of the pinch in the tube and the rigid outlet pipe(mm/s) with a P_{E2} of 800 Pa. Q = 1.66×10^{-6} (top), 8.3×10^{-6} (middle) and 1.66×10^{-5} (bottom) m^3 sec^{-1}.

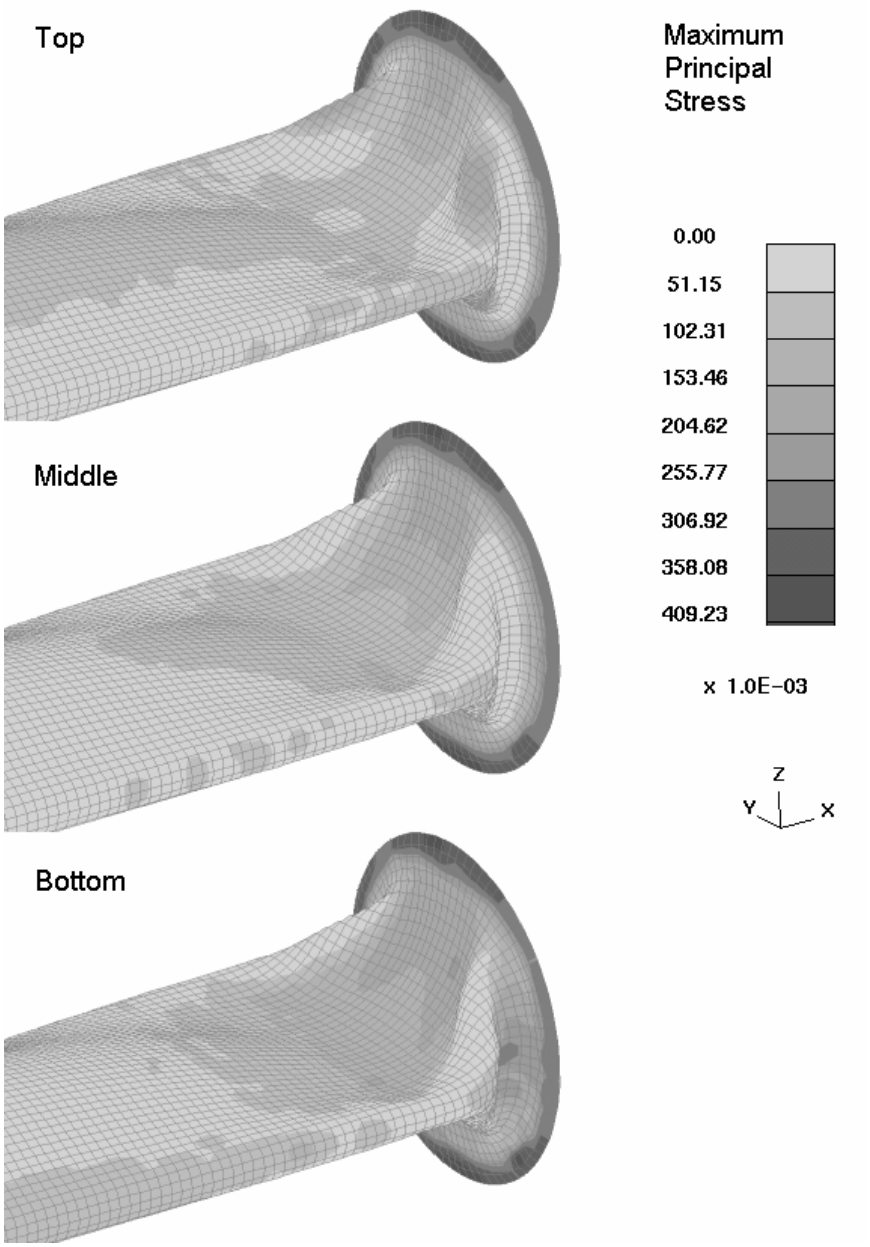

Figure 10. Maximum principal stress for the top, middle and bottom integration points of the collapsible tube with P_{E2} at 100 Pa and flow rate Q of 8.33×10^{-6} m^3 sec^{-1}.